

Microscopic theory of photoassisted field emission from metals

C. Caroli, D. Lederer-Rozenblatt, B. Roulet, and D. Saint-James

*Groupe de Physique des Solides de l'École Normale Supérieure,
Université Paris VII, 2 place Jussieu, 75221 Paris Cedex 05, France*

(Received 26 December 1973)

We derive a general microscopic expression for the photoassisted-field-emission current and the energy distribution curve (EDC) with the help of a nonequilibrium perturbation formalism. It is shown that, in spite of the irreversible nature of the (unperturbed) field-emission system, the EDC at energies above the Fermi level of the emitter is given by the same formal expression as in the pure photoemission case. This EDC is calculated in the simple case of a semi-infinite free-electron emitter. These results are used to discuss what information could be obtained from photoassisted-field-emission experiments concerning the shape of the surface potential and the electronic properties of the cathode.

I. INTRODUCTION

Photoemission (PE) and field emission (FE) have been recently the subject of much interest from both the experimental and the theoretical points of view. Developments in these two fields have been made possible by the considerable improvement of vacuum technology and of the quality of electron detectors. These two types of experiments share one essential feature—they measure currents that are extracted *out* of a solid, i.e., currents made up of electrons all of which have crossed the surface region. They are therefore good tools for probing surface properties of solids, e.g., work functions, surface states, adsorbed states, etc. Moreover, from the energy distribution curves (EDC), one also extracts information about the density of bulk electron states in the emitter. While field emission is due to electrons below the Fermi level μ ¹ and therefore probes the corresponding energy range, photoemission contains information about both the initial and final states of the photon absorption process. That is, it explores the two ranges $\epsilon < \mu$, since the initial state must be occupied, and $\epsilon > E$ (where E is the vacuum energy), since the final state must extend to infinity in the vacuum region in order for the corresponding electron to contribute to the photocurrent.

One is therefore left with an energy gap $\mu < \epsilon < E$ of width $\phi = E - \mu$ (ϕ is the work function of the material) typically of the order of a few eV, which neither photoemission nor field emission can probe. It is possible to reduce this gap, namely to lower the work function, by cesiating the emitting solid. However, on the one hand, ϕ cannot be lowered by more than about 2 eV; on the other hand, the surface states of the emitter are certainly modified by the presence of the Cs layer.

One is therefore led to the natural idea of combining photoemission and field emission into

photoassisted field emission² (PFE): a metal tip is illuminated with light of frequency Ω , the photo-excited electrons then give rise to a field-emission current in the energy range $\epsilon < \mu + \Omega$.³ Such experiments have recently been realized on tungsten⁴⁻⁶ in which both the total PFE current and its energy distribution are measured. These experiments have been interpreted on the basis of the three-step model of photoemission, which assumes that the current is the result of three independent (i.e., multiplicative) processes: optical absorption, propagation of the excited electron to the surface, and transmission into vacuum. When this model is applied to PFE, the static electric field is taken into account only in the last step, in which the transmission coefficient through the emission barrier is expressed by means of a Miller-Good- (or Nordheim-) type of formula.

Such an interpretation, although widely used to interpret photoemission data, has been proved recently,⁷⁻⁹ on the basis of first-principles calculation of the PE current, to have at most a qualitative value. Indeed, this appears when the photocurrent is correctly expressed as the (quadratic) response to the electromagnetic field. In PFE, the situation is complicated further, and the quadratic-response formalism must be extended to take into account the fact that the system in the absence of the optical field is out of equilibrium.

In Sec. II we derive the general expression for the energy distribution curve (EDC) of the elastic PFE current above the Fermi level, and discuss in detail the formal implications of the detailed balance of the charge distribution. In Sec. III we apply these results to the very simple case of a semi-infinite free-electron gas emitter and normally incident light. We obtain an expression of the elastic EDC which is valid whatever the precise shape of the surface barrier. The influence of this shape appears in the result only through a

single (energy-dependent) parameter which characterizes the reflectivity of the barrier. Finally, in Sec. IV we discuss briefly what kind of information one can reasonably hope to extract from PFE experiments in practical situations, in which one must take into account further complications due to the lattice structure and the various interaction effects.

II. FORMAL EXPRESSION OF THE CURRENT

Let us consider a semi-infinite metal at zero temperature, extending in the region $x < 0$, with a perfectly plane surface at $x = 0$, in the presence of a strong dc electric field $\vec{\mathcal{E}}$ normal to the surface. $\vec{\mathcal{E}}$ is zero in the metal (its penetration is negligible) and uniform in the vacuum region ($x > 0$). Let H_0 be the Hamiltonian of this system; we assume it to be an independent-electron Hamiltonian. This means that we neglect, in a first stage, interactions inside the metal (their influence will be discussed in Sec. IV) and that we describe the interaction between an electron in the vacuum and the metal by a one-electron potential $v(x)$.¹⁰ The simplest expression of $v(x)$ is the image potential one, $v(x) = -e^2/4x$; one can also use one of its various improved forms.¹¹ In the vacuum region, the electron is therefore submitted to the total potential

$$V(x) = E - e\mathcal{E}x + v(x), \quad (2.1)$$

where $E = \mu + \phi$ is the vacuum level. This potential has a barrier shape, its maximum value decreases when \mathcal{E} increases (Schottky effect).

This system is submitted to an electromagnetic field deriving from the vector potential

$$\vec{A}(\vec{r}, t) = \hat{y}a(x) \cos\Omega t, \quad (2.2)$$

i.e., we choose the gauge so that the scalar potential is zero, and we assume the field to be monochromatic, linearly polarized along direction \hat{y} parallel to the surface, and at normal incidence.¹² $a(x)$ is oscillating in the vacuum ($x > 0$) and decreases on a penetration depth δ in the solid ($x < 0$).

The coupling between the ac field and the electrons is described by the Hamiltonian

$$H_1 = \int d^3r \Psi^\dagger(\vec{r}t) \times \left(\frac{ie\hbar}{mc} \vec{A}(\vec{r}t) \cdot \vec{\nabla} + \frac{e^2}{2mc^2} [\vec{A}(\vec{r}, t)]^2 \right) \Psi(rt) \quad (2.3)$$

where $\Psi^\dagger(\vec{r}t)$ [$\Psi(\vec{r}t)$] are the electron creation [destruction] operators.

The total current density is given (for the two

spin directions) by

$$\vec{j}(\vec{r}t) = 2\hbar \left(\frac{e\hbar}{2m} (\vec{\nabla}_{\vec{r}'} - \vec{\nabla}_{\vec{r}}) + \frac{ie^2\vec{A}(\vec{r}, t)}{mc} \right) \times G_{\text{tot}}^+(\vec{r}t, \vec{r}'t) \Big|_{\vec{r}'=\vec{r}} \quad (2.4)$$

and

$$G_{\text{tot}}^+(\vec{r}t, \vec{r}'t) = i \langle \Psi^\dagger(\vec{r}'t) \Psi(\vec{r}t) \rangle \quad (2.5)$$

is a Green's function of the complete system, i.e., in the presence of both the ac and dc fields. G_{tot}^+ may be expanded in powers of the small-coupling Hamiltonian H_1 and, following what is done in photoemission,⁹ the terms in the resulting perturbation expansion are then classified and ordered into a power series in A , which reads

$$G_{\text{tot}}^+ = G^+ + G^{(1)+} + G^{(2)+} + \dots \quad (2.6)$$

But, contrary to what happens in ordinary photoemission, the unperturbed system to which the perturbation H_1 is applied is out of equilibrium. Indeed, due to the presence of the dc field, H_0 describes a field-emission system with a finite stationary current flow. Therefore, the zeroth-order system must be described within the frame of Keldysh's formalism (this has been done in Ref. 13), which must naturally also be used to perform the expansion (2.6).

Making use of Eqs. (2.6) and (2.4) we can also express the current as a power series in A :

$$\vec{j}(\vec{r}t) = \vec{j}^{(0)}(\vec{r}, t) + \vec{j}^{(1)}(\vec{r}, t) + \vec{j}^{(2)}(\vec{r}t) + \dots \quad (2.7)$$

The zeroth-order term $\vec{j}^{(0)}$ is the field-emission current flowing in the x direction, which has been calculated in Ref. 13. Note that $\vec{j}^{(0)}$ is a dc current and that its energy distribution is entirely concentrated in the range $\omega < \mu$. (This comes from the fact that, in our independent-electron model, there exists no physical process that can provide energy to excite electrons into states above the Fermi level of the cathode.¹⁴)

The first-order term $\vec{j}^{(1)}$ is the conductivity current of the field-emission system, it is therefore an ac current at the finite frequency Ω . Photo(assisted)-emission experiments only measure the dc part of j_x , so that $\vec{j}^{(1)}$ does not contribute to the assisted photocurrent.

The second-order term $\vec{j}^{(2)}$ contains two parts: (i) the "gauge current" $\vec{A}G^{(1)+}(\vec{r}t, \vec{r}t)$, which does not contribute to the PFE current, since it is parallel to the surface¹⁵; (ii) the only remaining term is simply

$$\vec{J}(\vec{r}, t) = \frac{e\hbar^2}{m} (\vec{\nabla}_{\vec{r}'} - \vec{\nabla}_{\vec{r}}) G^{(2)+}(\vec{r}t, \vec{r}'t) \Big|_{\vec{r}'=\vec{r}} \quad (2.8)$$

In order to simplify the following calculations, we shall assume the solid to have complete translational invariance in the yz plane. This condition—which is assumed to hold in most treatments of field emission—can be released without difficulty and periodicity effects can be included in the following formal calculation. However, taking them into account brings in such considerable algebraic complications (even in zeroth order, i.e., in the pure field-emission case) that it only seems possible to discuss their effects qualitatively on the basis of the results obtained in the simple case studied hereafter.

Then, the total photoassisted dc current flowing out of the surface has the same formal expression as in photoemission:

$$J_x = \int d\omega \mathcal{J}_x(\omega),$$

$$\begin{aligned} G_{\vec{q}\omega}^{(2)+}(x, x') = & \int dx_1 \frac{e^2 a^2(x_1)}{4m^2 c^2} [\hat{G}_{\vec{q}\omega}^+(xx_1) \hat{\sigma}_z \hat{G}_{\vec{q}\omega}^+(x_1 x')]^{(+ -)} \\ & + \frac{e^2 \hbar^2 q_y^2}{4m^2 c^2} \int dx_1 dx_2 a(x_1) a(x_2) \{ \hat{G}_{\vec{q}\omega}^+(xx_1) \hat{\sigma}_z [\hat{G}_{\vec{q}, \omega + \Omega}^+(x_1 x_2) + \hat{G}_{\vec{q}, \omega - \Omega}^+(x_1 x_2)] \hat{\sigma}_z \hat{G}_{\vec{q}\omega}^+(x_2 x') \}^{(+ -)}, \end{aligned} \quad (2.10)$$

where the notations are those of paper I, i.e.,

$$\hat{G} = \begin{pmatrix} G^c & G^+ \\ G^- & \bar{G}^c \end{pmatrix} \text{ and } \hat{\sigma}_z = \begin{pmatrix} 1 & 0 \\ 0 & -1 \end{pmatrix},$$

and $(+ -)$ means the first-line, second-column term of the matrix product.

The first term of the right-hand side of Eq. (2.10) comes from the diamagnetic part of the electromagnetic perturbation acting to first order.

We will show now that this term (which is zero in the PE case) is finite, due to presence of the finite FE current in the unperturbed system. Indeed, it is proportional to

$$G_{\vec{q}\omega}^+(xx_1) G_{\vec{q}\omega}^+(x_1 x') + G_{\vec{q}\omega}^+(xx_1) G_{\vec{q}\omega}^+(x_1 x'). \quad (2.11)$$

Here, as in the PE case, the zeroth-order electron occupation propagators G^+ are strictly zero for $\omega > \mu$. This means that, as we have pointed out above, the field-emission current is distributed only in the $\omega < \mu$ energy range.

On the other hand, the current is measured at infinity from the sample, i.e., the relevant x and

where the EDC is given by

$$\begin{aligned} \mathcal{J}_x(\omega) = & \frac{1}{2\pi} \int \frac{d^2 q}{(2\pi)^2} \frac{e \hbar^2}{m} \left(\frac{\partial}{\partial x'} - \frac{\partial}{\partial x} \right) \\ & \times G_{\vec{q}\omega}^{(2)+}(x, x') \Big|_{x'=x(=\infty)}, \end{aligned} \quad (2.9)$$

with

$$\begin{aligned} G_{\vec{q}\omega}^{(2)+}(x, x') = & \int d^2 \rho dt dt' G^{(2)+}(\vec{r}t, \vec{r}'t') \\ & \times \exp[i\vec{q} \cdot (\vec{\rho} - \vec{\rho}') - i\omega(t - t')] \end{aligned}$$

and $\vec{\rho}$ is a vector of the yz plane.

The formal Keldysh perturbation expansion which gives $G^{(2)+}$ in terms of the zeroth-order Green's matrix \hat{G} then proceeds exactly as in the photoemission case, i.e., we get [see Eq. (10) of Ref. 9, hereafter referred to as paper I]

x' in (2.10) $\rightarrow +\infty$. In PE, the advanced and retarded propagators G^a and G^r in (2.11), as well as the G^+ , are then zero for $\omega < \mu$ (in other words, electrons at energies below the vacuum level cannot escape from the solid). Here, on the contrary, $\lim_{x \rightarrow \infty} G_{\vec{q}\omega}^+(x_1 x) \neq 0$ for $\omega < \mu$. Indeed, due to the presence of the FE current an electron in any occupied level has a finite [although exponentially decreasing with decreasing $\omega - \epsilon_q (= \omega - \hbar^2 q^2 / 2m)$] probability of tunneling from the solid into the vacuum.

Therefore the corresponding "diamagnetic" current is now finite, but its EDC is concentrated below the Fermi level. Thus it simply gives a small correction [$\sim A^2 j^{(0)}(\omega)$] to the field emission EDC $j^{(0)}(\omega)$.

It does not seem of much interest to study PFE in that energy range ($\omega < \mu$) which is already explored (much more easily) by FE. Consequently we will specialize from now on to the region $\omega > \mu$, and we can ignore the diamagnetic contribution.

We are then left with

$$\begin{aligned} \mathcal{J}_x(\omega) = & \frac{1}{2\pi} \int \frac{d^2 q}{(2\pi)^2} \frac{1}{4} \left(\frac{e \hbar q_y}{mc} \right)^2 \frac{e \hbar^2}{m} \left(\frac{\partial}{\partial x'} - \frac{\partial}{\partial x} \right) \int dx_1 dx_2 a(x_1) a(x_2) \\ & \times \{ \hat{G}_{\vec{q}\omega}^+(x, x_1) \hat{\sigma}_z [\hat{G}_{\vec{q}, \omega + \Omega}^+(x_1, x_2) + \hat{G}_{\vec{q}, \omega - \Omega}^+(x_1, x_2)] \hat{\sigma}_z \hat{G}_{\vec{q}\omega}^+(x_2, x') \}^{(+ -)} \Big|_{x'=x(=\infty)}. \end{aligned} \quad (2.12)$$

Developing the matrix product, and taking into account that, for $\omega > \mu$

$$G_{\bar{q}\omega}^{\pm}(x, x') = G_{\bar{q}, \omega + \Omega}^{\pm}(x, x') = 0,$$

we obtain

$$\mathcal{J}_x(\omega) = \frac{1}{2\pi} \int \frac{d^2q}{(2\pi)^2} \frac{1}{4} \left(\frac{e\hbar q}{mc} \right)^2 \frac{e\hbar^2}{m} \left(\frac{\partial}{\partial x'} - \frac{\partial}{\partial x} \right) \int dx_1 dx_2 a(x_1) a(x_2) G_{\bar{q}\omega}^r(x, x_1) G_{\bar{q}, \omega - \Omega}^{\pm}(x_1, x_2) G_{\bar{q}\omega}^a(x_2, x') \Big|_{x'=x(=\infty)}, \quad \omega > \mu. \quad (2.13)$$

Equation (2.13) means that the EDC $\mathcal{J}_x(\omega)$ is due to electrons which were occupying states of energy $\omega - \Omega$ in the unperturbed system (factor $G_{\bar{q}, \omega - \Omega}^{\pm}$) and have been optically excited to the final level ω (factor $G_{\bar{q}\omega}^r G_{\bar{q}\omega}^a$). Since $G_{\bar{q}, \omega - \Omega}^{\pm} \propto \theta(\mu - \omega + \Omega)$, $\mathcal{J}_x(\omega)$ is limited, as it should be, to the region $\omega < \mu + \Omega$. This expression is formally identical to the PE one [Eq. (14) of paper I], but here the G 's are those of the field-emission situation. They must be calculated by the method developed in Ref. 13 and this will be done in detail for a specific model in the next section.

Before going into such explicit calculations one question must be raised: when writing down Eqs. (2.9), (2.12), and (2.13), we have implicitly taken for granted that the EDC $\mathcal{J}_x(\omega)$ is independent of

the position of the point x where it is measured. This point is of course assumed, as in plain photoemission, to be infinitely far from the sample ($x = +\infty$) in order for the collecting apparatus not to perturb the system under study.

This assumes that the quantity $\mathcal{J}_x(\omega, x)$ of Eq. (2.13), when first calculated for finite x , has a well-defined limit when $x \rightarrow \infty$. In order to check whether this is the case, let us calculate $\vec{\nabla} \cdot \vec{\mathcal{J}}(\omega, x) = \partial \mathcal{J}_x(\omega, x) / \partial x$. Making use of Eq. (2.13) and of the equation of motion of the $G^{a,r}$'s,

$$\left[\omega - \epsilon_{\bar{q}} + \frac{\hbar^2}{2m} \frac{d^2}{dx^2} - V(x) \right] G_{\bar{q}, \omega}^{r,a}(x, x') = \delta(x - x'), \quad (2.14)$$

we get

$$\frac{\partial \mathcal{J}_x(\omega, x)}{\partial x} = \frac{a(x)}{2\pi} \int \frac{d^2q}{(2\pi)^2} \frac{e\hbar^2}{m} \left(\frac{e\hbar q_y}{mc} \right)^2 \frac{1}{4} \frac{2m}{\hbar^2} \int dx_1 a(x_1) [G_{\bar{q}, \omega - \Omega}^{\pm}(x_1, x) G_{\bar{q}\omega}^r(x, x_1) - G_{\bar{q}, \omega - \Omega}^{\pm}(x, x_1) G_{\bar{q}\omega}^a(x_1, x)]. \quad (2.15)$$

On the other hand, we can define (to the same order in A) the electromagnetic power absorbed per unit volume of the system at point x , as

$$\bar{P}(x) = \langle \vec{E} \cdot \vec{J}^{(1)} \rangle$$

where $\vec{E} = -(1/c) \partial \vec{A} / \partial t$, $\vec{J}^{(1)}(\vec{r}, t)$ is the conductivity current (i.e., is given by a first-order response expression) and $\langle \rangle$ indicates time averaging. We thus obtain

$$\bar{P} = \hbar \Omega \int d\omega \varphi(\omega, x),$$

with

$$\varphi(\omega, x) = \frac{a(x)}{2\pi} \int \frac{d^2q}{(2\pi)^2} \frac{1}{2} \left(\frac{e\hbar q_y}{mc} \right)^2 \int dx_1 a(x_1) [\hat{G}_{\bar{q}, \omega - \Omega}(x, x_1) \hat{\sigma}_z \hat{G}_{\bar{q}\omega}(x_1, x) - \hat{G}_{\bar{q}\omega}(x, x_1) \hat{\sigma}_z \hat{G}_{\bar{q}, \omega - \Omega}(x_1, x)]^{(+ -)}. \quad (2.16)$$

For $\omega > \mu$, this expression reduces to

$$\varphi(\omega, x) = \frac{a(x)}{2\pi} \int \frac{d^2q}{(2\pi)^2} \frac{1}{2} \left(\frac{e\hbar q_y}{mc} \right)^2 \int dx_1 a(x_1) [G_{\bar{q}, \omega - \Omega}^{\pm}(x, x_1) G_{\bar{q}\omega}^a(x_1, x) - G_{\bar{q}\omega}^r(x, x_1) G_{\bar{q}, \omega - \Omega}^{\pm}(x_1, x)]. \quad (2.17)$$

It is clear from Eqs. (2.16) and (2.17) that $\varphi(\omega, x) \times d\omega dx$ can be interpreted to be the flux of electrons flowing per unit time into the energy range $(\omega, \omega + d\omega)$ in the volume element $(x, x + dx)$, due to optical transitions $\omega - \Omega - \omega$, each of which is associated with an energy absorption $\hbar \Omega$.

Comparing Eqs. (2.15) and (2.17) we see that

$$\vec{\nabla} \cdot \vec{\mathcal{J}}(\omega, x) + e\varphi(\omega, x) = 0 \quad (2.18)$$

(this relation can be shown to hold as well for $\omega < \mu$). Relation (2.18) simply expresses that the local energy distribution of particles $N(\omega, x)$ obeys a detailed balance principle, even in the presence of the field-emission current.

It is obvious from Eq. (2.18) that $\partial \mathcal{J}(\omega, x)/\partial x$ is nonzero in any region of space where the density of electrons at energy $\omega - \Omega$ (and thus the optical transition probability) of the unperturbed system is nonzero. In the PE situation, there are no electrons at infinity in the vacuum [$\lim_{x \rightarrow \infty} G_{\omega - \Omega}^+(xx_1) = 0$] so that $\lim_{x \rightarrow \infty} \partial \mathcal{J}(\omega, x)/\partial x = 0$, and the photocurrent $\lim_{x \rightarrow \infty} \mathcal{J}(\omega, x)$ is uniquely defined. The situation is different in PFE: indeed, an electron density exists even at infinity in the vacuum, due to the presence of the field-emission current. This means that $\partial \mathcal{J}(\omega, x)/\partial x$ is nonzero, even for $x \rightarrow \infty$, so that one cannot, in principle, uniquely define a PFE current.

This result appears of course to be somewhat paradoxical. There are in fact two ways of avoiding the difficulty.

(i) The "practical" one: one calculates explicitly $\mathcal{J}(\omega, x)$ from Eq. (2.13) for a specific model (e.g., the one of Sec. III). One then finds that, for $x \rightarrow \infty$, $\mathcal{J}_x(\omega, x) \rightarrow \mathcal{J}_x(\omega) + f_{osc}(x^{3/2})$, where the oscillating function f_{osc} has an amplitude $\sim j^{(0)}(\omega)A^2$ and its local "wavelength" goes to zero when $x \rightarrow \infty$.¹⁶ Since, in a real experiment the collector (and the emitting surface) are not ideal planes, there is a finite uncertainty Δx on the measuring point, and the oscillating term in $\mathcal{J}(\omega, x)$ averages to zero, and it is in practice the average value $\mathcal{J}(\omega)$ which is detected.

(ii) The "conceptual" one: in the PFE situation, the "system" which is submitted to the perturbation extends wherever there is a finite electron density, i.e., up to the collector of the field-emission current. Quite obviously, in order for the measured (PFE) current to characterize the response of the whole system under study, the measuring apparatus (PFE collector) must be outside of this system. Conceptually, this can be realized in the following setup: the FE collecting filter is at $x = X_1$, the PFE one at $x = X_1 + X_2$, with very large X_1 and X_2 (note that this device is possible because we are only interested in the PFE current energy distribution above μ). Then $\varphi(\omega, X_1 + X_2)$ in Eq. (2.18) is zero, and $\mathcal{J}_x(\omega)$ is uniquely defined.

In practical calculations, one must therefore use the following recipe (which we apply in the next section): make $x > x_1$ and x_2 in Eq. (2.13) (even when x_1 and $x_2 \rightarrow \infty$).

III. PFE FROM A FREE-ELECTRON METAL

As stated in Sec. II, we restrict our calculation of the EDC to the region $\omega > \mu$, where $\mathcal{J}_x(\omega)$ is given by Eq. (2.13). We assume that the emitting metal is a semi-infinite free-electron gas extending in the region $x < 0$ [where the potential

$V(x) = 0$]. However, we do not make any assumption about the detailed shape of the surface barrier. Note that the interaction potential between an electron in vacuum and the metal $v(x)$ goes to zero when $x \rightarrow \infty$, so that

$$V(x) \underset{x \rightarrow \infty}{\sim} E - e\mathcal{E}x$$

independently of the approximation one may choose for $v(x)$.

$V(x)$ is represented schematically in Fig. 1. We now have to calculate the G 's of the field-emission system which appear in Eq. (2.13).

G^a and G^r are simply dynamical functions which do not contain any information about the thermodynamics of the system. They can therefore be calculated by solving the equation of motion (2.14), subject to the boundary condition that $G_{\vec{q}\omega}^a$ ($G_{\vec{q}\omega}^r$) be analytical in the lower (upper) half ω plane.

Let us define two functions $\psi_{\vec{q}\omega}^r(x)$ and $\varphi_{\vec{q}\omega}^r$ by the following conditions:

(i) they are solutions of the Schrödinger equation of our system

$$\left(\omega - \epsilon_{\vec{q}} + \frac{\hbar^2}{2m} \frac{d^2}{dx^2} - V(x)\right) \varphi_{\vec{q}\omega}^r(x) = 0, \quad (3.1a)$$

$$\left(\omega - \epsilon_{\vec{q}} + \frac{\hbar^2}{2m} \frac{d^2}{dx^2} - V(x)\right) \psi_{\vec{q}\omega}^r = 0; \quad (3.1b)$$

(ii) $\psi_{\vec{q}\omega}^r(x)$ behaves as a pure outgoing wave towards positive x when $x \rightarrow +\infty$. $\varphi_{\vec{q}\omega}^r(x)$ is a pure outgoing wave towards negative x when $x \rightarrow -\infty$. Then one may write

$$G_{\vec{q}\omega}^r(x, x') = \frac{2m}{\hbar^2} \frac{\varphi_{\vec{q}\omega}^r(x_<) \psi_{\vec{q}\omega}^r(x_>)}{\varphi_{\vec{q}\omega}^r(0) \psi_{\vec{q}\omega}^r(0) - \varphi_{\vec{q}\omega}^r(0) \psi_{\vec{q}\omega}^r(0)} = [G_{\vec{q}\omega}^a(x, x')]^* \quad (3.2)$$

In the metal region ($x < 0$) we can take

$$\varphi_{\vec{q}\omega}^r(x) = e^{-ikx}, \quad (3.3)$$

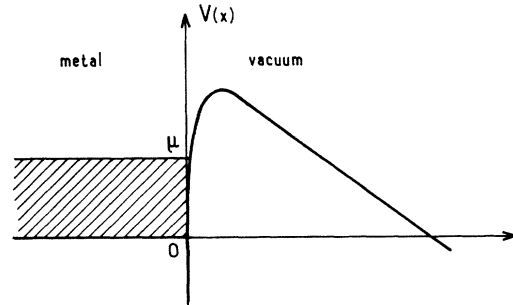


FIG. 1. Schematic representation of the potential barrier.

where

$$k \equiv k(\bar{q}, \omega) = [(2m/\hbar^2)(\omega - \epsilon_{\bar{q}})]^{1/2} \quad (3.3)$$

and we define ψ^r by its asymptotic behavior at infinity in the vacuum, namely

$$\psi_{\bar{q}\omega}^r \underset{x \rightarrow \infty}{\sim} \frac{2me\delta(x - x_0)}{\hbar^2} e^{-i/4} \times \exp\left[\frac{2i}{3} \left(\frac{2me\delta}{\hbar^2} (x - x_0)^3\right)^{1/2}\right], \quad (3.4)$$

where $x_0 = [E - (\omega - \epsilon_{\bar{q}})]/e\delta$.

We now define the transmission and reflexion coefficients (at transverse energy $\omega - \epsilon_{\bar{q}}$) by

$$T_{\bar{q}\omega}^r = \frac{2ik\psi_{\bar{q}\omega}^r(0)}{ik\psi_{\bar{q}\omega}^r(0) + \psi_{\bar{q}\omega}^{r'}(0)}, \quad (3.5)$$

$$R_{\bar{q}\omega}^r = 1 - T_{\bar{q}\omega}^r = (R_{\bar{q}\omega}^a)^*.$$

We can then write explicitly G^r as

$$G_{\bar{q}\omega}^r(x, x') = \frac{2m}{\hbar^2} \frac{1}{2ik} (e^{ikhx} - R_{\bar{q}\omega}^r e^{-ikhx}) e^{-ikhx} \text{ for } x \text{ and } x' \leq 0$$

$$= \frac{2m}{\hbar^2} \frac{T_{\bar{q}\omega}^r}{2ik} e^{-ikhx'} \frac{\psi_{\bar{q}\omega}^r(x)}{\psi_{\bar{q}\omega}^r(0)} \text{ for } x' \leq 0 \leq x$$

$$= \frac{2m}{\hbar^2} \frac{T_{\bar{q}\omega}^r}{2ik} \varphi_{\bar{q}\omega}^r(x_<) \frac{\psi_{\bar{q}\omega}^r(x_>)}{\psi_{\bar{q}\omega}^r(0)} \text{ for } x \text{ and } x' > 0. \quad (3.6)$$

and $G_{\bar{q}\omega}^a$ is given by the same expressions with subscript a substituted for r .

These expressions for the dynamical functions G^a and G^r are independent of the thermodynamic state of the system, and all the statistical information in Eq. (2.13) about the departure from equilibrium is contained in the electron occupation propagator $G_{\bar{q}, \omega - \Omega}^{\pm}(x_1, x_2)$. This propagator we calculate with the help of the method that we have developed in Ref. 17 (see also Refs. 13 and 18). Let us simply recall here that in this method one expresses the properties of the current-carrying system in terms of those of two semi-infinite media, most naturally identified here with the metal electrode ($x < 0$) and the vacuum ($x > 0$). Each of these media is separately at equilibrium, with chemical potentials μ (for the metal) and $-\infty$ (for the vacuum).

Using the kind of algebraic manipulation of Ref. 17, and reexpressing the expressions thus obtained for G^+ in terms of G^a and G^r , we obtain¹⁸

$$G_{\bar{q}\omega}^{\pm}(x_1, x_2) = \theta(-x_1)G_{\bar{q}\omega}^a(x_1, x_2) - \theta(-x_2)G_{\bar{q}\omega}^r(x_1, x_2)$$

$$+ \frac{\hbar^2}{2m} [G_{\bar{q}\omega}^r(x_1, 0)G_{\bar{q}\omega}^a(0, x_2)$$

$$- G_{\bar{q}\omega}^{r'}(x_1, 0)G_{\bar{q}\omega}^a(0, x_2)], \quad (3.7)$$

where

$$G_{\bar{q}\omega}^{r'}(x_1, 0) = \frac{\partial}{\partial x} G_{\bar{q}\omega}^r(x_1, x) \Big|_{x=0}.$$

Note that expression (3.7) is valid whatever the shape of the one-dimensional potential $V(x)$, provided that the electron occupation propagator g_R^+ of the right-hand ($x > 0$) semi-infinite isolated subsystem is strictly zero at all values of the energy.

Finally, neglecting the (optical) wavelength of the electromagnetic field, we take

$$a(x) = a = \text{constant}, \quad x > 0$$

$$= ae^{x/\delta}, \quad x < 0. \quad (3.8)$$

Making use of Eqs. (2.13) and (3.6)–(3.8) and taking advantage of the fact that

$$\int_0^{\infty} \psi_{\bar{q}\omega}^r(x) \varphi_{\bar{q}\omega}^r(x) dx = \frac{\hbar^2}{2m(\omega' - \omega)}$$

$$\times (\psi_{\bar{q}\omega}^{r'} \varphi_{\bar{q}\omega}^r - \psi_{\bar{q}\omega}^r \varphi_{\bar{q}\omega}^{r'})_{x=0}, \quad (3.9)$$

we obtain for the photoassisted EDC above the metal Fermi level

$$\dot{J}_x(\omega) = \frac{a^2}{2\pi} \theta(\mu + \Omega - \omega) \int \frac{d^2q}{(2\pi)^2} \theta(\omega - \Omega - \epsilon_{\bar{q}}) \frac{e\hbar^2}{m} \left(\frac{2m}{\hbar^2}\right)^3 \left(\frac{e\hbar q_x}{2mc}\right)^2$$

$$\times (1 - R_{\bar{q}\omega}^r R_{\bar{q}\omega}^a) \frac{1}{4kk'} \left| \frac{1}{\delta^{-1} - i(k - k')} + \frac{R_{\bar{q}\omega}^{r'}}{\delta^{-1} - i(k + k')} - i \left(\frac{1}{k - k'} + \frac{R_{\bar{q}\omega}^r}{k + k'} \right) \right|^2, \quad (3.10)$$

with $\omega' \equiv \omega - \Omega$ and $k' \equiv k(\vec{q}, \omega') = [(2m/\hbar^2) \times (\omega - \Omega - \epsilon_{\vec{q}})]^{1/2}$.

We can first remark that, when $\delta \rightarrow \infty$, $\mathcal{J}_x(\omega) \rightarrow 0$; that is, the current is not affected by the presence of the electromagnetic field. This feature is well known in photoemission, where several authors have shown that no PE current can flow in this oversimplified model. The physical reason for it is the following: assuming $a(x) = \text{constant}$ amounts to neglecting the ac magnetic field. Then, since we also neglect the lattice potential in the metal, the motion of an electron along x and (yz), respectively, is separable (in particular there is no Lorentz force). Therefore the ac electric field which is parallel to the surface cannot induce any modification of the current in the x direction.

The quantity $\mathcal{T}_{\vec{q}\omega} = (1 - R_{\vec{q}\omega}^r R_{\vec{q}\omega}^a)$ characterizes the "transparency" of the barrier at energy ω , for electrons of parallel wave vector \vec{q} . Indeed, should electron states at energy ω in the metal be occupied, the corresponding FE current density would read¹⁹

$$\mathcal{J}_{\vec{q}\omega}^{(0)} = \frac{1}{2\pi} \int \frac{d^2q}{(2\pi)^2} \frac{e\hbar^2}{m} \frac{2m}{\hbar^2} (1 - R_{\vec{q}\omega}^r R_{\vec{q}\omega}^a). \quad (3.11)$$

Let us now examine the remaining factors in Eq. (3.10). k and k' are slowly varying functions of the energy. On the other hand, when $\delta \rightarrow 0$, at transverse energies $\omega - \epsilon_{\vec{q}} < E$, $\psi_{\vec{q}\omega}(x)$ is real and Eq. (3.5) shows that $|R_{\vec{q}\omega}^r| \rightarrow 1$. As can be seen from Eq. (3.11), this amounts to saying that the field-emission EDC decreases exponentially when the barrier thickness increases. The reflection coefficient $R_{\vec{q}, \omega - \Omega}$ which appears in the last factor of Eq. (3.10) corresponds to states below the Fermi level, for which the barrier transparency is very small. Therefore, $R_{\vec{q}\omega}^r$ can be approxi-

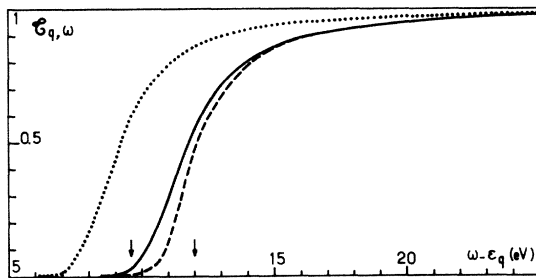


FIG. 2. The "transparency" coefficient $\mathcal{T}_{\vec{q}\omega}$ versus $(\omega - \epsilon_{\vec{q}})$ for different triangular barriers; $V(x) = E - e\mathcal{E}x$. The solid and dashed curves correspond, respectively, to $\mathcal{E} = 0.7 \text{ V/\AA}$ and $\mathcal{E} = 0.38 \text{ V/\AA}$, with $E = 12 \text{ eV}$. The dotted curve corresponds to $\mathcal{E} = 0.7 \text{ V/\AA}$ with $E = 9.6 \text{ eV}$ (which would be the value of V_{max} in the image potential model for the chosen \mathcal{E}). The arrows refer to the two values of E .

mated reasonably by its value in zero static electric field, which is a slowly varying function of ω . This can be illustrated by the case of the Fowler-Nordheim triangular-barrier model, where

$$R_{\vec{q}\omega}^r \approx \frac{ik' + (E - \omega' + \epsilon_{\vec{q}})^{1/2}}{ik' - (E - \omega' + \epsilon_{\vec{q}})^{1/2}} + \frac{4k'(E - \omega' + \epsilon_{\vec{q}})^{1/2}}{[ik' - (E - \omega' + \epsilon_{\vec{q}})^{1/2}]^2} \times \exp \left\{ -\frac{4}{3e\mathcal{E}} \left(\frac{2m}{\hbar^2} (E - \omega' + \epsilon_{\vec{q}})^3 \right)^{1/2} \right\}. \quad (3.12)$$

Therefore, the variation of the photoassisted-field-emission EDC with ω , at fixed \mathcal{E} and Ω , is essentially controlled by the variation of the transparency coefficient in the final state. The general behavior of $\mathcal{T}_{\vec{q}\omega} = 1 - R_{\vec{q}\omega}^r R_{\vec{q}\omega}^a$ is the following.

It is an increasing function of $(\omega - \epsilon_{\vec{q}})$. At low energies, for

$$x_0 \gg \left(\frac{2m}{\hbar^2} [V_{\text{max}}(\mathcal{E}) - \omega + \epsilon_{\vec{q}}] \right)^{-1/2}$$

[where x_0 is the barrier thickness at energy $\omega - \epsilon_{\vec{q}}$, and $V_{\text{max}}(\mathcal{E})$ is the potential at the top of the barrier], it is exponentially small, as expected from the usual field-emission results. It increases rapidly in the "transitional" range $\omega - \epsilon_{\vec{q}} \sim V_{\text{max}}$, then, in the "photoelectric" range $\omega - \epsilon_{\vec{q}} \gg V_{\text{max}}$, it varies slowly towards its limit $\mathcal{T}_{(\omega - \epsilon_{\vec{q}} = \infty)} = 1$.

This behavior is illustrated on Fig. 2, where we plot $\mathcal{T}_{\vec{q}\omega}$ for the Fowler-Nordheim triangular barrier for two different values of \mathcal{E} and V_{max} , respectively.

Let us, however, insist that in order to obtain the EDC $\mathcal{J}_x(\omega)$, one needs to integrate the contributions of all q 's such that $0 < \epsilon_{\vec{q}} < \omega - \Omega$. This will result in a further broadening of the transitional region of the EDC, the practical implications of which are discussed in the next section.

IV. QUALITATIVE FEATURES OF PFE FROM REAL METALS

Up to now, we have neglected all interaction effects inside the cathode. In real metals, as in photoemission, these effects cannot actually be neglected, since the excitation energy in the final states of interest is greater than about 1–2 eV. At such energies, the mean free path $l(\omega)$ is typically of a few hundred \AA . This limits the extraction depth of the elastic current and gives rise to an inelastic contribution to the EDC. This can be included into the formal treatment of Sec. II in exactly the same way as has been done for photoemission (see paper I). It is then found that if the self-energy is quasilocal, the elastic EDC (for an interacting free-electron cathode) is given by Eq. (3.10), provided one replaces δ by the

elastic extraction depth $L = (\delta^{-1} + l^{-1})^{-1}$. The measured EDC also includes an inelastic contribution, the losses are due to emission of phonons and/or electron-hole pairs. They have been discussed in detail in paper I. Let us simply recall that, as for PE in the optical range, the upper part of the EDC (in a range of ~ 1 eV below the maximum energy $\mu + \Omega$) is essentially due to the elastic current and to electrons which have emitted a few phonons. This gives rise to a broadening of the possible structures of the order of a few tenths of an eV. The lower part of EDC curves, where electron-hole losses are important, is in general very difficult to interpret.

Note, however, that the contribution to the total current J_x^{tot} of electrons which have created electron-hole pairs should be quite small: this arises from the fact that, due to the increase of the barrier thickness with decreasing energy, the relative weight in J_x of the low-energy part of $\mathcal{J}_x(\omega)$ is exponentially small compared to the weight of the upper part.

There are in principle two categories of information one can hope to extract from PFE experiments. (i) The first one is concerned with the shape of the surface barrier close to the metal surface. In particular, one would like⁴⁻⁶ to measure its maximum height as a function of the static electric field, and, if possible, detect deviations from the prediction of the simple unscreened image potential model, which gives

$$V_{\text{max}}^{(\text{im})}(\mathcal{E}) = E - (e^3 \mathcal{E})^{1/2}. \quad (4.1)$$

(ii) The second one deals with the structure and density of electronic states in the range $\mu < \omega < E$, including possible surface states.

It is clear that in order to study the barrier shape one must, as far as possible, choose a material with a regular shape of the density-of-states curve: indeed, as can be inferred from Eq. (3.10), the condition for the variation of the EDC with ω to be controlled by the transparency in the final state is that all other terms—i.e., all propagation properties inside the cathode—vary smoothly with energy. Assuming that this condition is fulfilled, we can examine point (i) on the qualitative basis of Eq. (3.10) (with $\delta^{-1} \sim L^{-1}$).

Three ways of studying the barrier top can be contemplated.

EDC measurements at constant \mathcal{E} and Ω in the energy range around $V_{\text{max}}(\mathcal{E})$: Such experiments are of course technically very difficult to realize, due to the smallness of the signal. One should then choose a value of Ω such that $\mu + \Omega \sim V_{\text{max}} + \frac{1}{2}$ eV, in order to avoid having too large an inelastic EDC at $\omega \sim V_{\text{max}}$.

Total PFE current J_x versus \mathcal{E} at constant Ω ⁴⁻⁶:

In our model, J_x is obtained by integrating expression (3.10). Strictly speaking, as shown in Sec. II, one should use a different expression for $\omega < \mu$. However, the transparency coefficient at such energies is very small compared with the one of the highest excited states, and this effect can be neglected. Ω must be chosen so that $0 < E - (\mu + \Omega) \lesssim 1$ eV. In principle, one hopes to see a rapid variation of J_x when V_{max} decreases below $\mu + \Omega$.

Total PFE current versus Ω at constant \mathcal{E} : This could be realized with the help, for instance, of tunable dye laser. It would then be of most interest to plot the quantity $\partial J_x / \partial \Omega$ versus Ω . Indeed, as far as there is no very sharp electronic structure of the initial states, the variation with Ω of the last factor of (3.10) is slow and $\partial J_x / \partial \Omega$ should not differ very much from $\mathcal{J}_x(\mu + \Omega)$, i.e., from the uppermost part of the EDC, which is practically elastic.

Following the discussion of Sec. II it may be seen that all such experiments measure the variation with energy of some \bar{q} average of the transparency coefficient in the final state.

As shown on Fig. 2, $\mathcal{T}_{\bar{q}\omega}$ has no singularity for $\omega - \epsilon_{\bar{q}} = V_{\text{max}}$ and the change from the exponential (tunneling) regime to the "photoelectric" one takes place on a range $\Delta(\omega - \epsilon_{\bar{q}})$, typically of the order of 2 eV. Moreover, the width of this transitional region increases when the averaging over parallel wave vectors is performed. This averaging smoothes the whole structure of the $\mathcal{T}_{\bar{q}\omega}$ curve, so that one cannot expect to get very accurate information about $V_{\text{max}}(\mathcal{E})$ from the study of a single EDC. However, as is illustrated by the oversimplified model of Fig. 2, the transparency-coefficient curves for constant V_{max} are not very sensitive to variations of the electric field. Consequently, a change of \mathcal{E} in a real system, i.e., with a corresponding change in V_{max} , results in a deformation of the \mathcal{T} -vs- $(\omega - \epsilon_{\bar{q}})$ curve which, in the transitional range, reduces practically to a translation $\Delta(\omega - \epsilon_{\bar{q}}) = \Delta V_{\text{max}}$.

It can therefore be concluded that the study of a single EDC can only detect the change from the tunneling to the photoelectric regime, and does not provide an accurate determination of the absolute value of V_{max} . However, it would be of interest to study a set of EDC's measured at different values of the static field, since the shift of the transitional region of these curves should give reasonably accurate information on the variations of V_{max} with \mathcal{E} .

Finally, let us consider point (ii). The discussion that can be made on that point is very similar to that which has been made in paper I for PE. We will thus only emphasize a few important remarks. Information about the final electron states

cannot be properly extracted from a measurement of the current J_e ,²⁰ but only of the EDC. The "step model," as in photoemission, cannot be deduced from the microscopic calculation, and must be considered to be only of qualitative value. At the energies of interest ($\omega < V_{\max}$), the matching conditions for wave functions at the surface are certainly of even more crucial importance than in PE. Indeed, the effective barrier thickness, i.e., the transparency coefficient $\mathcal{T}_{\vec{q}\omega}$ varies with \vec{q} much more rapidly than does the transmission coefficient in the energy range ($\omega > E$) of interest in PE.

Getting more than these semiquantitative informations about both the surface and the electronic structure of the cathode below vacuum level would be at the moment very difficult. Indeed, in order to go one step further than the present analysis, it would be necessary to extend the present microscopic calculation to include lattice effects (in the presence of a surface) and to compute the EDC thus obtained for various models of the barrier shape. Completing such a task will perhaps be feasible when such computations will have been performed and checked in the simpler photoemission situation.

*Laboratoire associé au Centre National de la Recherche Scientifique.

¹We neglect temperature effects, since in usual experimental situations the temperature is negligible compared with the extraction work—which is the natural energy scale for field emission—as well as the very small Auger tails above the Fermi energy.

²B. I. Lundquist, K. Mountfield, and J. W. Wilkins, *Solid State Commun.* **10**, 383 (1972).

³These states can also be explored by thermal field emission, which probes preferentially a region of ~ 1 – 2 eV above μ , since heating is limited by the thermal stability of the tip.

⁴Martin J. G. Lee, *Phys. Rev. Lett.* **30**, 1193 (1973).

⁵H. Neumann and Ch. Kleint, *Ann. Phys. (Leipz.)* **27**, 237 (1971).

⁶Y. Teisseyre, R. Coelho, and R. Haug, *C. R. Acad. Sci. Paris* **274**, 1202 (1972).

⁷G. D. Mahan, *Phys. Rev. B* **2**, 4334 (1970).

⁸W. L. Schaich and N. W. Ashcroft, *Phys. Rev. B* **3**, 2452 (1971).

⁹C. Caroli, D. Lederer-Rozenblatt, B. Roulet, and D. Saint-James, *Phys. Rev. B* **8**, 4552 (1973). This paper will hereafter be referred to as paper I.

¹⁰This neglects the fact that, at distances of atomic order from the surface, the interaction potential is nonlocal and retarded.

¹¹See, for instance, P. H. Cutler and J. C. Davis, *Surf. Sci.* **1**, 194 (1964).

¹²In fact, as long as the field is linearly polarized along a direction parallel to the surface, the incidence angle

plays no role on the result. For a study of PFE at non-normal incidence and in a free-electron model, see A. Bagchi, *Phys. Rev.* (to be published).

¹³C. Caroli, D. Lederer, and D. Saint-James, *Surf. Sci.* **33**, 228 (1972).

¹⁴When for instance, electron-electron interactions in the metal are taken into account, it is found that Auger processes may take place in the current-carrying system, which give rise to nonzero tails of the distribution of the field-emission current above μ .

¹⁵In the case when \vec{A} is not parallel to the surface, this term gives a nonzero contribution to the PFE (while it is zero in simple photoemission), but it can legitimately be neglected, since its ratio to the total PFE current is $\sim (\mu/\Omega) \cdot (a/\delta)$, where a is the atomic distance in the solid.

¹⁶This behavior is controlled by the behavior of the wave functions at infinity in the vacuum, and is therefore independent of the model chosen to describe the solid.

¹⁷C. Caroli, R. Combescot, D. Lederer, P. Nozières, and D. Saint-James, *J. Phys. C* **4**, 2598 (1971).

¹⁸D. Lederer-Rozenblatt, thesis (Université de Paris VII, Paris, 1974) (unpublished).

¹⁹Equation (3.10) is identical to Eq. (12) of Ref. 13, since, in the notations of Ref. 13

$$1 - R_{\vec{q}\omega}^{\uparrow} R_{\vec{q}\omega}^{\downarrow} = -4 \frac{\text{Im}\gamma_{\vec{q}\omega}^{\uparrow} \text{Im}\gamma_{\vec{q}\omega}^{\downarrow}}{|\gamma_{\vec{q}\omega}^{\uparrow} + \gamma_{\vec{q}\omega}^{\downarrow}|^2}.$$

²⁰Except maybe if small static fields are used, in which case the surface barrier itself may provide the high-pass filter.